Biomechanical, Morphological, and Biochemical Characteristics of Articular Cartilage of the Ovine Humeral Head

Erin McCready[1], Jeremiah T. Easley[1], Makayla Risch[1], Kevin L. Troyer[2], James W. Johnson[2], Benjamin C. Gadomski[2], Kirk C. McGilvray[2], John D. Kisiday[3], and Brad B. Nelson[1,3] (iD)

Abstract

Objective. Shoulder pain is commonly attributed to rotator cuff injury or osteoarthritis. Ovine translational models are used to investigate novel treatments aimed at remedying these conditions to prevent articular cartilage degeneration and subsequent joint degradation. However, topographical properties of articular cartilage in the ovine shoulder are undefined. This study investigates the biomechanical, morphological, and biochemical attributes of healthy ovine humeral head articular cartilage and characterizes topographical variations between surface locations. *Design.* Ten humeral heads were collected from healthy skeletally mature sheep and each was segregated into 4 quadrants using 16 regions of interest (ROIs) across the articular surface. Articular cartilage of each ROI was analyzed for creep indentation, thickness, and sulfated glycosaminoglycan (sGAG) and collagen quantity. Comparisons of each variable were made between quadrants and between ROIs within each quadrant. *Results.* Percent creep, thickness, and sGAG content, but not collagen content, were significantly different between humeral head quadrants. Subregion analysis of the ROIs within each surface quadrant revealed differences in all measured variables within at least one quadrant. Percent creep was correlated with sGAG (r = −0.32, *P* = 0.0001). Collagen content was correlated with percent creep (r = 0.32, *P* = 0.0009), sGAG (r = −0.19, *P* = 0.049), and thickness (r = −0.19, *P* = 0.04). *Conclusions.* Topographical variations exist in mechanical, morphologic, and biochemical properties across the articular surface of the ovine humeral head. Recognizing this variability in ovine humeral head cartilage will provide researchers and clinicians with accurate information that could impact study outcomes.

Keywords

articular cartilage, computed tomography, shoulder, collagen, glycosaminoglycans

Introduction

Shoulder pain is a common disorder with the cause frequently attributed to acute or chronic rotator cuff injury or osteoarthritis in the aging population.[1] Approximately 30% of patients with rotator cuff tears have concurrent articular cartilage injury of the glenohumeral joint[2-4] and the prevalence of glenohumeral osteoarthritis has been estimated as high as 26%.[5] Articular cartilage damage leads to the development and furthers the progression of osteoarthritis, persisting shoulder pain. New treatment strategies are being pursued in translational large animal models to improve rotator cuff repair prior to incorporation into human clinical trials.[6-11] However, these studies largely focus on healing of the humeral tendon-bone enthesis and typically neglecting the neighboring articular cartilage.

[1]Preclinical Surgical Research Laboratory, C. Wayne McIlwraith Translational Medicine Institute, Department of Clinical Sciences, Colorado State University, Fort Collins, CO, USA
[2]Orthopaedic Bioengineering Research Laboratory, Department of Mechanical Engineering, Colorado State University, Fort Collins, CO, USA
[3]Orthopaedic Research Center, C. Wayne McIlwraith Translational Medicine Institute, Department of Clinical Sciences, Colorado State University, Fort Collins, CO, USA

Supplementary material for this article is available on the *Cartilage* website at http://cart.sagepub.com/supplemental.

Corresponding Author:
Brad B. Nelson, Preclinical Surgical Research Laboratory, C. Wayne McIlwraith Translational Medicine Institute, Department of Clinical Sciences, Colorado State University, 300 W. Drake Road, Fort Collins, CO 80523, USA.
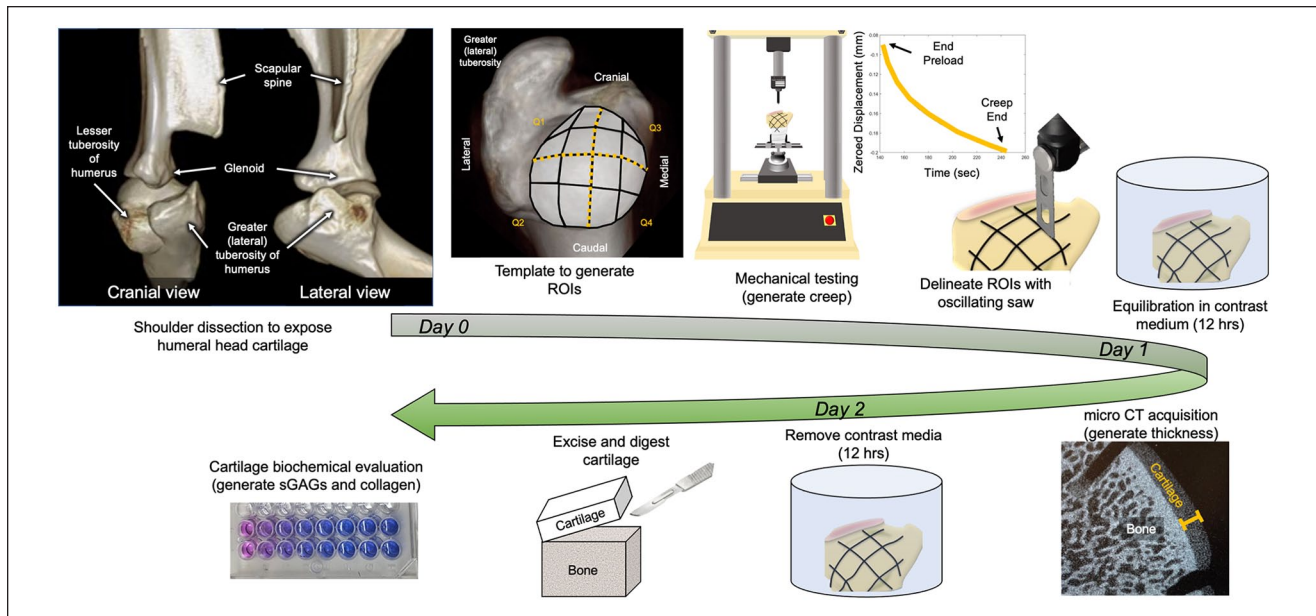Email: Brad.nelson@colostate.edu

Figure 1. Experimental methods and timeline. Q = quadrant; ROIs = regions of interest; sGAGs, sulfated glycosaminoglycans; CT = computed tomography.

Ovine orthopedic models offer an opportunity to investigate novel cartilage healing and rotator cuff repair approaches due to their similar joint size and body weight as humans.[6-8,12] Articular cartilage has different compositional attributes across surfaces to accommodate for particular demands within the joint, which is recognized across human and animal joints.[13-18] Due to comparative musculoskeletal features across mammalian species, the site of preclinical testing in research animals is frequently adapted to the anatomically analogous site in humans. For example, the stifle (knee) joint in sheep is commonly used for preclinical testing of devices intended for use in human knees.[19-22] Despite the common use of ovine preclinical shoulder models to translate these data to humans, there are no data on the topography of ovine humeral head cartilage. Enhanced knowledge of ovine cartilage properties will optimize the implementation of human-designed medical devices and therapies researched in sheep and will improve the accuracy of translation to humans in forthcoming clinical trials.

The objectives of this study were to describe the mechanical, morphological, and biochemical properties from ovine humeral head cartilage and delineate differences in those attributes as they exist across the articular surface. We hypothesized that there will be topographical differences in these properties between and within surface locations of ovine humeral head cartilage.

Methods

Study Design and Sample Harvest

Ten glenohumeral joints (5 left, 5 right) were collected from 10 skeletally mature (3+ years of age) Rambouillet cross-breed ewes euthanized for reasons unrelated to shoulder joint disease. Shoulders were frozen with surrounding soft tissue intact at −20 °C until the day before testing. Prior to testing, specimens were allowed to thaw completely at room temperature without compromising tissue integrity in the planned analyses.[23,24] After thawing, soft tissue dissection was performed to expose the joint surface. Gross examination of the articular surface of the humeral head was performed, and any shoulder joint surfaces with macroscopic articular cartilage or bone abnormalities were excluded. In the first 10 joints examined, none were excluded due to these criteria. A reusable mesh overlay constructed from a pliable fabric was created to evenly divide the entire articular surface of the humeral head into 16 approximately 1 cm² regions of interest (ROIs) during testing. The same mesh overlay was applied to each joint surface and examined to ensure consistent locations were tested across specimens. Joint surface quadrants were established by grouping the ROIs (4 per quadrant) to depict anatomically distinct locations (quadrant 1: craniolateral aspect, quadrant 2: caudolateral, quadrant 3: craniomedial, and quadrant 4: caudomedial) (**Fig. 1**). A total of 160 ROIs (from all 10 limbs) were available for subsequent analysis. The articular cartilage from each ROI was analyzed for its mechanical (creep indentation), morphological (articular cartilage thickness), and biochemical (sulfated glycosaminoglycan [sGAG] and collagen) properties.

Mechanical Testing

Mechanical evaluation was accomplished using macro indentation on the intact articular surface.[8,20] The intact humeral head was secured into a multiaxial vice ensuring

even contact between the articular cartilage and the indenter tip (perpendicular to the load axis). Testing was performed under force control using a 3-mm hemispherical indenter attached to a 100 N load cell and servohydraulic material testing system (MTS 858, Mini Bionix II, Scotia, NY).[19] Hydration of articular cartilage was maintained during testing using a 400 mOsm preservative saline solution that contained nonspecific protease inhibitors, antibiotics, and antimycotics (5 mM Benzamidine HCl, 5 mM EDTA, Sigma-Aldrich, St. Louis, MO; 1x Antibiotic-Antimycotic, Life Tech, Carlsbad, CA) to minimize autolysis during testing. Each test was performed by placing the actuator perpendicular to the ROI (approximately 2 mm from the surface) and then ramped at a rate of .025 mm/s until a pre-load of .05 N was achieved. The preload was held for 100 seconds, after which the load was increased at a rate of .1 N/s to .8 N and allowed to creep for 100 seconds.[19] The recovery curve data (displacement vs. time) were used to calculate percent creep at each ROI. Creep was normalized to the measured displacement during testing at the end of preload to account for variation between samples.[19] Following mechanical testing, an oscillating saw was used to score samples along the template lines into the subchondral bone plate thus physically delineating and enabling accuracy of each ROI for each subsequent analysis.

Articular Cartilage Thickness Assessment

En bloc humeral heads were equilibrated for 12 hours in an iodinated contrast medium solution (24 mg iodine/mL, Omnipaque, GE Healthcare, Milwaukee, WI). Following equilibration, the samples were placed into the µCT scanning chamber (µCT80; Scanco Medical, Brüttisellen).[19,25] All samples were scanned in the same orientation. Preservative saline-soaked gauze was placed in the scanning chambers, which were then sealed with paraffin wax to prevent articular cartilage desiccation during scanning. The µCT scan (µCT80; Scanco Medical) was completed at 20 μm^3 voxel dimensions with 70 kVp energy, 114 µA intensity, and 300 ms integration time. Average cartilage thickness of each ROI was determined by measuring the distance from the subchondral bone perpendicular to the articular surface at 5 random locations within each given ROI by a single investigator with 7 years of quantitative imaging analysis expertise, and all measurements were performed on the same day. The 5 measurements were averaged to provide a mean articular cartilage thickness at each ROI. Measurements were obtained using commercially available software (Scanco Evaluator application; Scanco Medical).

Biochemical Assays

Following µCT imaging, the humeral head was submerged overnight in a 500 mL bath containing the preservative saline solution to remove contrast media prior to biochemical testing. This approach has been shown to extract contrast media from the articular cartilage.[25] The articular cartilage from each ROI was excised from the subchondral bone using a scalpel blade. Resulting cartilage samples from each ROI were then weighed to obtain a hydrated (wet) weight, lyophilized for 24 hours, and reweighed to determine a dry weight. Samples were stored at −80 °C until all 160 samples were collected and could be analyzed simultaneously. The lyophilized samples were digested overnight in a proteinase K solution (100 µg/mL, Fisher Scientific, Hampton, NH) at 60 °C. Once particulate samples were fully digested, the sGAG and total collagen content of each sample were quantified using a 1,9-dimethylmethylene blue binding assay (DMMB)[26,27] and a hydroxyproline assay,[28,29] respectively. For sGAG quantification, samples were analyzed in triplicate and evaluated on a microplate reader (SpectraMax M3; Molecular Devices, Sunnyvale, CA) at 530 nm. Samples were averaged and compared with a standard curve of chondroitin sulfate C (C6737; Sigma-Aldrich, St. Louis, MO). Samples with $R^2 < .95$ or a coefficient of variation >10% between replicates were re-analyzed. The sGAG content of each ROI was reported as a mean and normalized to the wet weight of the sample. For collagen analysis, samples were hydrolyzed in 12.1 N HCl for 16 hours at 110°C and then evaporated on a heating block at 60°C overnight. Samples, along with known hydroxyproline standard concentrations, were plated in duplicate. Chloramine T reagent (50 mM, 857319, Sigma-Aldrich) was added and incubated for 20 minutes at 25°C. Then, the 4-dimethyl-aminobenzaldehyde reagent (1 M, 156477, Sigma-Aldrich) was added and incubated at 60°C for 15 minutes followed by 5 minutes at 25°C. The plates were then read at 550 nm. Hydroxyproline concentrations for each sample were determined from the standard curve. Total collagen was determined using an established conversion (8.2 mg hydroxyproline/mg collagen)[30] recorded as a mean and standardized to tissue dry weight.

Data and Statistical Analysis

Continuous data were represented as mean ± SD. For each variable, comparisons were made between quadrants using a mixed model analysis. Fixed effects included surface quadrant, ROI, and surface quadrant*ROI interaction. Limb number and limb number × surface quadrant were random effects to account for repeated measures. Tukey-Kramer adjustments were applied to account for bias from multiple comparisons. Mixed model analysis assumptions were assessed based on visual inspection of residual diagnostic plots. Correlations between parameters were calculated accounting for repeated measures on subjects[31] and correlation strength characterized (slight: 0-.2, fair: .21-.4, moderate: .41-.6, strong: .61-.8, very
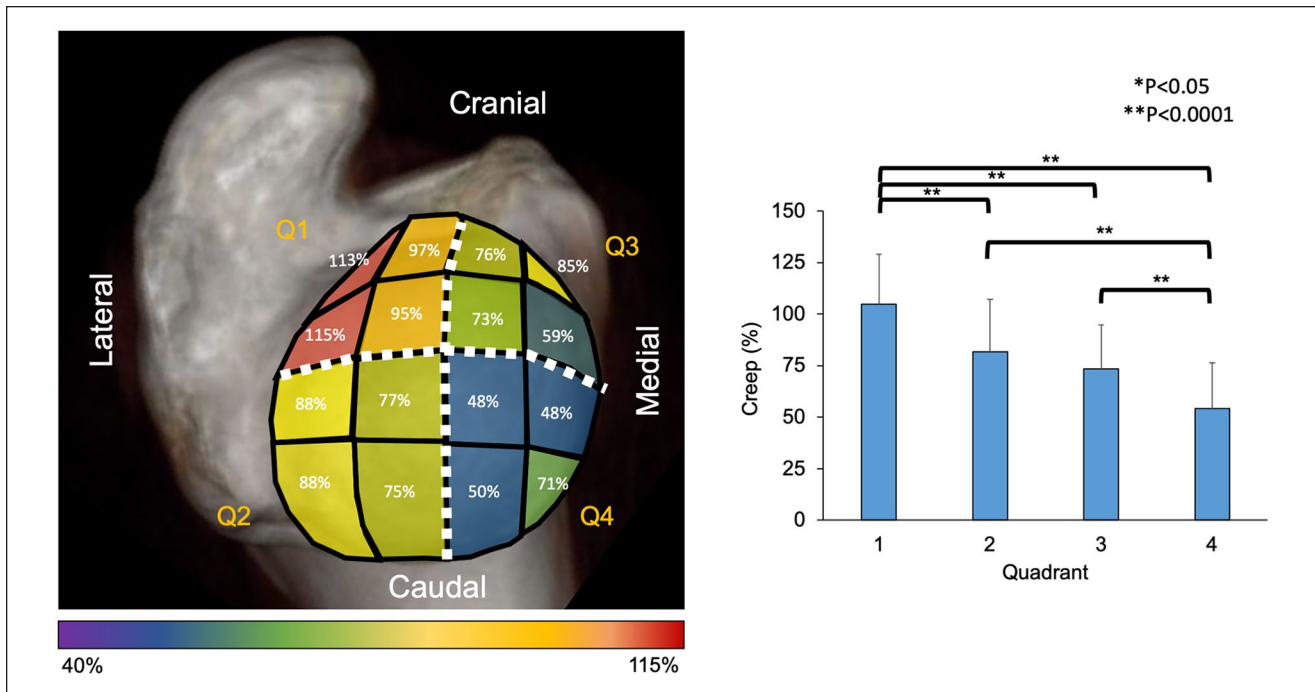
Figure 2. Topographical distribution of percent creep of articular cartilage across the ovine humeral head. The mean values are reported along with an applied color map displaying the range of values (left). The histogram (right) represents overall comparisons made between quadrants. Data values are mean ± standard deviation. Q = quadrant.

strong: .81-1.0).[32] Statistical analyses were accomplished using SAS (SAS University Edition, v9.2; SAS Institute Inc., Cary, NC) and significance was defined at $P < 0.05$.

Results

Mean percent creep values ranged from 48% to 115% and the overall average of all ROIs was 78% ± 29% (**Fig. 2**). Mean percent creep at quadrant 1 (105% ± 24%) was significantly higher than quadrant 2 (82% ± 25%, $P < 0.0001$), quadrant 3 (73% ± 21%, $P < 0.0001$), and quadrant 4 (54% ± 22%, $P < 0.0001$). Mean percent creep in quadrant 4 was significantly lower than quadrant 2 and quadrant 3 (both $P < 0.0001$). There were significant differences among ROIs within quadrant 1 ($P = 0.04$), quadrant 3 ($P = 0.034$), and quadrant 4 ($P = 0.04$) (Suppl. Fig. S1).

Mean articular cartilage thickness values ranged from 0.66 to 0.92 mm and the overall average of all ROIs was 0.79 mm ± 0.13 mm (**Fig. 3**). Mean thickness at quadrant 1 (0.739 mm ± 0.120 mm) was significantly thinner than quadrant 2 (0.810 mm ± 0.132 mm, $P = 0.006$) and quadrant 4 (0.862 mm ± 0.121 mm, $P < 0.0001$). The thickness in quadrant 4 was significantly thicker than quadrant 2 ($P = 0.039$) and quadrant 3 (0.758 mm ± 0.103 mm, $P < 0.0001$). Mean articular cartilage thickness in quadrant 2 was thicker than quadrant 3 ($P = 0.045$). There were significant differences among ROIs within quadrant 1

($P = 0.020$), quadrant 2 ($P = 0.0006$), and quadrant 4 ($P = 0.005$) (Suppl. Fig. S1).

Mean sGAG content values ranged from 1.9% to 4.8% wet weight and the overall average of all ROIs was 3.4% ± 1.6% (**Fig. 4**). Mean sGAG content at quadrant 4 (3.9% ± 1.8%) was significantly higher than quadrant 1 (2.8% ± 1.3%, $P = 0.0005$) and quadrant 3 (3.3% ± 1.5%, $P < 0.05$). There were significant differences among ROIs within quadrant 1 ($P = 0.003$), quadrant 3 ($P < 0.0001$), and quadrant 4 ($P = 0.007$) (Suppl. Fig. S1).

Mean collagen content values ranged from 25% to 42% dry weight and the overall average of all ROIs was 34% ± 16% dry weight (**Fig. 5**). There were significant differences among ROIs within quadrant 2 ($P = 0.037$) (Suppl. Fig. S1).

There was a fair correlation between collagen content and creep (r = 0.32, $P = 0.0009$), a slight negative correlation between collagen content and sGAG (r = −0.19, $P = 0.049$), and between collagen content and thickness (r = −0.19, $P = 0.04$). There was a fair negative correlation between creep and sGAG (r = 0.32, $P = 0.0001$).

Discussion

This study characterized the topographical properties of ovine humeral head cartilage and revealed that locations across the surface vary in their mechanical, morphologic,
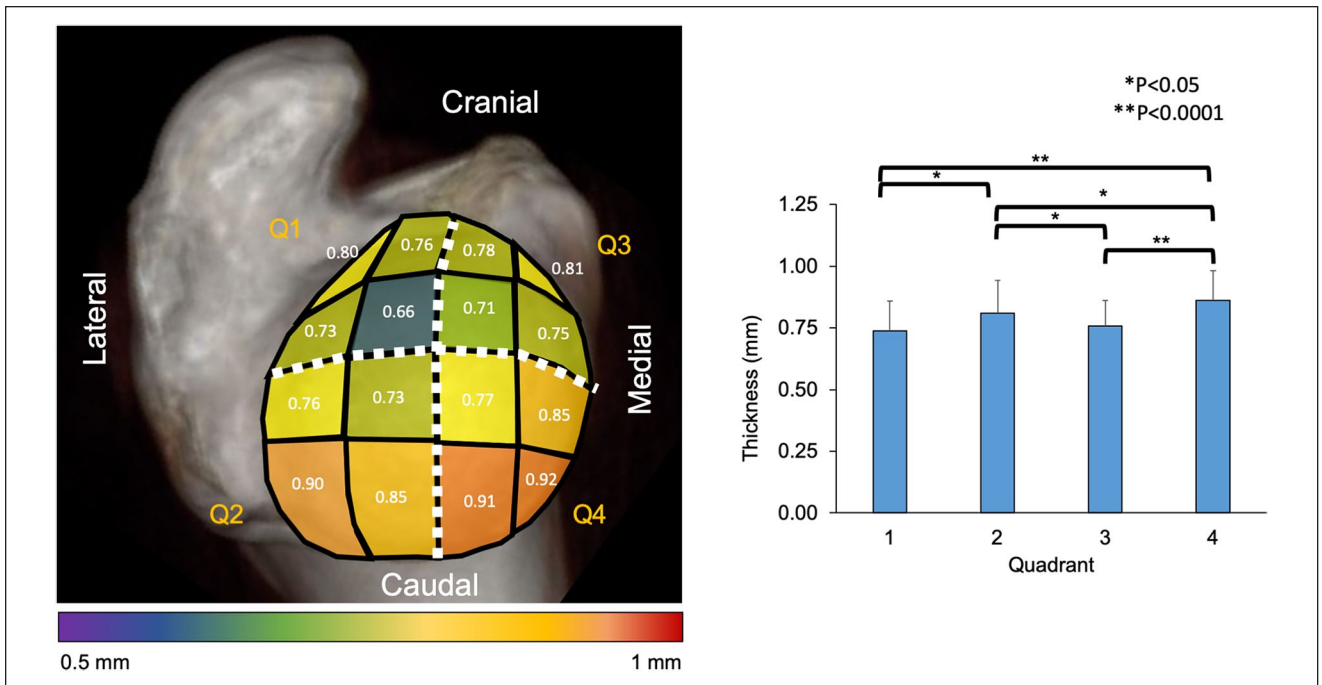
Figure 3. Topographical distribution of articular cartilage thickness of articular cartilage across the ovine humeral head. The mean values are reported along with an applied color map displaying the range of values (left). The histogram (right) represents overall comparisons made between quadrants. Data values are mean ± standard deviation. Q = quadrant.
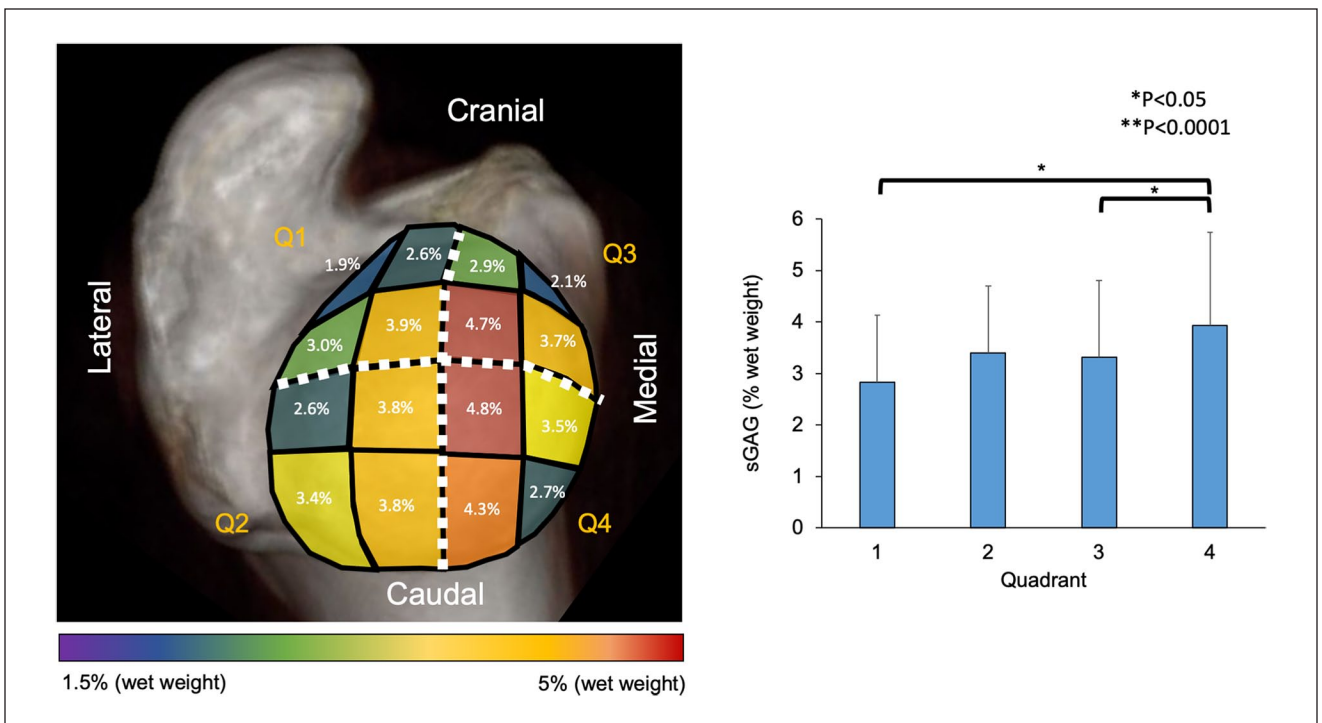

Figure 4. Topographical distribution of glycosaminoglycan (sulfated glycosaminoglycans) content of articular cartilage across the ovine humeral head. The mean values are reported along with an applied color map displaying the range of values (left). The histogram (right) represents overall comparisons made between quadrants. Data values are mean ± standard deviation. Q = quadrant.
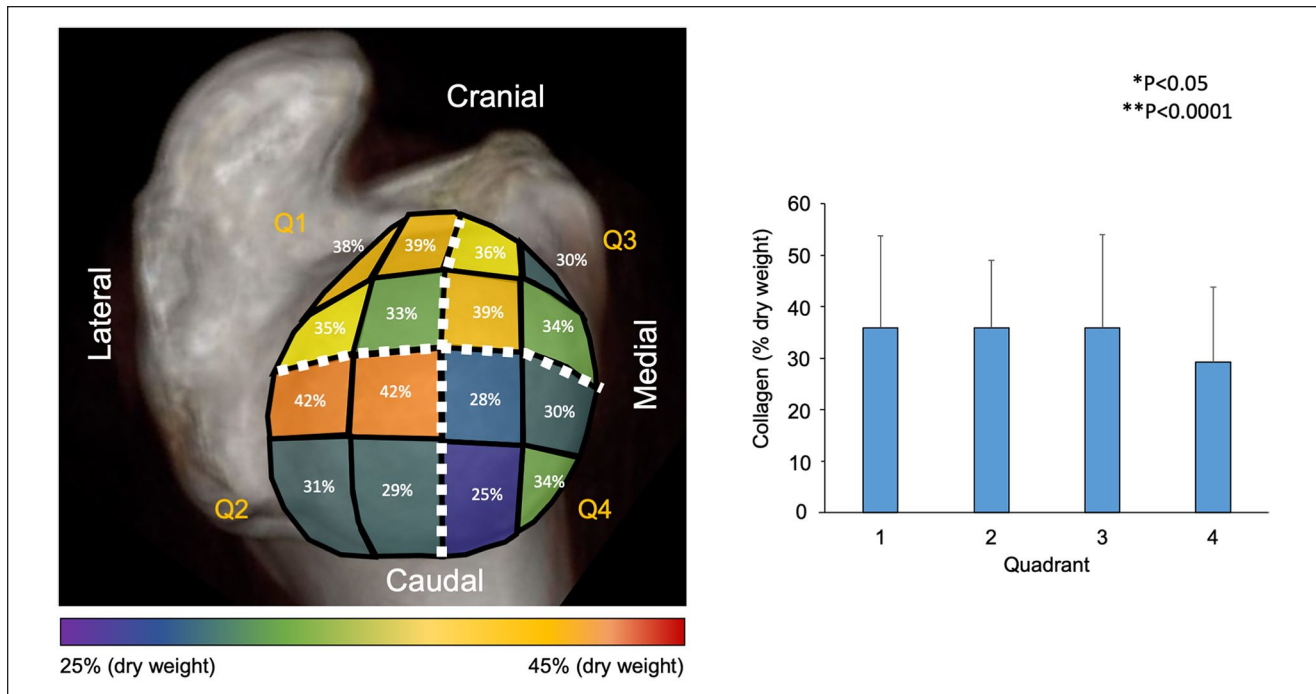
Figure 5. Topographical distribution of collagen content of articular cartilage across the ovine humeral head. The mean values are reported along with an applied color map displaying the range of values (left). The histogram (right) represents overall comparisons made between quadrants. Data values are mean ± standard deviation. Q = quadrant.

and biochemical attributes. The frequency of concurrent articular cartilage damage in rotator cuff injury and the prevalence of shoulder osteoarthritis raises awareness of the quality and integrity of this joint tissue in preclinical studies. In part, the data from this study supported our hypothesis. We found that mean percent creep, thickness, and sGAG content, but not collagen content, of articular cartilage of the humeral head varied between surface quadrants. In addition, subregion analysis of the ROIs within each surface quadrant revealed differences in all variables within at least one quadrant.

Thickness of ovine cartilage varied across the surface, while variation in human humeral head cartilage thickness has been reported.[33-38] Generally, articular cartilage thickness of the humeral head in humans (average 1.2 mm)[35,39] is thicker than was measured from sheep in this study (average 0.79 mm). In this study, cartilage thickness was significantly different between quadrants, though the mean difference between ROIs in our study was 0.1 to 0.2 mm (~12%-27% of average thickness), whereas 0.5 to 0.8 mm difference (~42%-66% of average thickness) has been reported in humans.[35] The thickest portion of humeral head cartilage in humans is localized to the central and superior portions.[35,40] In this study, the central portion was not the thickest and the caudal portion (analogous to the posterior location in humans) had slightly thicker cartilage relative to other locations. Despite these nuances, varying methods are

used to measure cartilage thickness in human and animal models challenging the direct comparisons between studies.[18,35,39] Variability in resolution and processing of the used method, whether it be needle penetration, MRI, micro–computed tomography (micro-CT), or histology,[16,17,19,41-43] can influence outcomes and comparisons between studies should be made recognizing this caveat.

Proteoglycan quantity varied across the surface of the ovine humeral head. The central and caudal (posterior) portions had the highest sGAG content on a wet weight basis. These findings could suggest that higher areas of weight bearing loads may occur at these locations compared with the anterior surface. However, the positive correlation between sGAG content and stiffer cartilage is observed in some,[5,44] but not all studies.[45] This inconsistency could be attributed to variations among animals and joints used or other cartilage constituents that influence the mechanical behavior of cartilage. Using this identical methodology and age-, sex-, and breed-matched sheep used in this study,[19] sGAG quantity of articular cartilage in the ovine knee was similar to the humeral head. The similar proteoglycan density between ovine knee and shoulder cartilage could be explained by the quadrupedal stature of sheep, where thoracic and pelvic limbs both experience weight-bearing loads. However, sGAG values are also similar between human shoulder and knee cartilage.[13,18] In humans, proteoglycan type but not the amount varies between joints.[13]

Shoulder joint cartilage has larger proteoglycans with increased chondroitin sulfate-rich regions compared with the knee and hip.[13] Proteoglycan types as they exist in non-human mammalian joints require further investigation. Despite structural differences observed on safranin-O histology, sGAG quantity and synthesis are not different between human knee, ankle, and shoulder joint cartilage.[18] Chubinskaya *et al.*[18] reported that sGAG quantity normalized to DNA content was higher in articular cartilage of the humeral head and glenoid when compared with the distal femur or talus, though this did not reach statistical significance.[18] Notably, these studies[13,18] report sGAG as a global representation or single site over the surface and do not take into account the topographical distribution. The inequalities of methods used to measure sGAG and normalization practices limit accurate comparisons between studies.

Biomechanical variation in cartilage occurs across the ovine humeral head. The mechanical behavior of articular cartilage is complex—displaying anisotropy, inhomogeneity, and tension-compression nonlinearity—with some studies reporting aggregate or equilibrium compressive modulus and others reporting creep.[19,41,46,47] While creep represents cartilage deformation at a constant load (with lower values indicating less deformation and a higher resistance to loading), aggregate modulus represents cartilage stiffness at equilibrium (higher values indicate less deformation and a higher resistance to loading). We chose to measure creep as a measure of mechanical behavior of cartilage as this identical methodology was used by our group previously for topographic mapping[19] and would enable consistent comparisons between those data and this study. Although this methodology enabled efficiency to perform multiple assessments on the same ROI, allowed us to capture differences in mechanical properties and an ability to directly compare data,[19] creep values do not solely represent the complex mechanical behavior of cartilage.[48,49] The central portion of ovine humeral head cartilage varied from 48% to 95% creep and the craniolateral quadrant had the highest mean percent creep, relative to the other sites. The caudomedial aspect of sheep humeral head cartilage had the lowest mean percent creep, whereas the central portion in humans[46] had the highest reported compressive modulus. In human cadaveric joints, articular cartilage evaluation of material (compressive) constants is different between glenoid and humeral head sites.[46] While the anterior surface of the humeral head had lower compressive modulus and the central region had the highest mean compressive modulus, direct comparisons within humeral head sites were not clearly outlined in this human cadaveric study.[46] The topographical differences between studies could be attributed to slight variations in mechanical testing protocols, bipedal versus quadrupedal stature of the species, or variations in articular cartilage thickness and composition of the underlying subchondral bone.

Topographical variations were observed in this study, though there are limitations to these data. Healthy, skeletally mature ewes were used to characterize cartilage and the determination of cartilage integrity was ascertained by visual inspection and through scrutiny of the outcome measures collected. Nonetheless, subtle degeneration may have gone unnoticed. Many of the studies using human joints use this same process to define healthy cartilage despite collection of cadaveric tissues from an aged population.[46,47] The limited availability of young human glenohumeral cartilage in research challenges the ability to make accurate age-matched comparisons between species. Considering the frequency of shoulder osteoarthritis and that human cadaveric samples are usually obtained from older donors, early degenerative cartilage could be mistaken for healthy using macroscopic evaluation alone. In this study, a statistically significant difference was observed between quadrants and among ROIs within quadrants, though statistical differences do not equate to biological differences and the magnitude of these changes must be interpreted in context with how these data are used.

Preclinical ovine models of orthopedic disease are prevalent in medical research and these data define articular cartilage properties across the surface of the ovine humeral head. Therapeutic interventions or medical devices that are optimized for addressing degenerative cartilage or that rely on specific mechanical or biochemical attributes of cartilage adjacent to the device would benefit to integrate this information, ensuring that study objectives are applicable to the translational model used. Noting the variations in mechanical, structural, and biochemical properties across the articular surface will improve our understanding of ovine cartilage in orthopedic research, ensuring that these attributes are considered for the optimization of future experimental studies.

Declaration of Conflicting Interests

The author(s) declared no potential conflicts of interest with respect to the research, authorship, and/or publication of this article.

Ethical Approval

Cadaver tissues obtained from other studies were used in all experiments. Specific approval for this study was not required. All animal use in those prior studies adhered to the ethical guidelines approved by the Institutional Animal Care and Use Committee at Colorado State University.

ORCID iD

Brad B. Nelson https://orcid.org/0000-0002-0205-418X

References

1. Zaid MB, Young NM, Pedoia V, Feeley BT, Ma CB, Lansdown DA. Anatomic shoulder parameters and their relationship to the presence of degenerative rotator cuff tears and glenohumeral osteoarthritis: a systematic review and meta-analysis. J Shoulder Elbow Surg. 2019;28:2457–66.

2. Spencer BA, Dolinskas CA, Seymour PA, Thomas SJ, Abboud JA. Glenohumeral articular cartilage lesions: prospective comparison of non-contrast magnetic resonance imaging and findings at arthroscopy. Arthroscopy. 2013;29:1466–70.

3. VanBeek C, Loeffler BJ, Narzikul A, Gordon V, Rasiej MJ, Kazam JK, et al. Diagnostic accuracy of noncontrast MRI for detection of glenohumeral cartilage lesions: a prospective comparison to arthroscopy. J Shoulder Elbow Surg. 2014;23:1010–6.

4. Krych AJ, Sousa PL, King AH, Morgan JA, May JH, Dahm DL. The effect of cartilage injury after arthroscopic stabilization for shoulder instability. Orthopedics. 2015;38:e965–99.

5. Thomas M, Bidwai A, Rangan A, Rees JL, Brownson P, Tennent D, et al. Glenohumeral osteoarthritis. Shoulder Elbow. 2016;8:203–14.

6. Easley J, Puttlitz C, Hackett E, Broomfield C, Nakamura L, Hawes M, et al. A prospective study comparing tendon-to-bone interface healing using an interposition bioresorbable scaffold with a vented anchor for primary rotator cuff repair in sheep. J Shoulder Elbow Surg. 2020;29:157–66.

7. Coleman SH, Fealy S, Ehteshami JR, MacGillivray JD, Altchek DW, Warren RF, et al. Chronic rotator cuff injury and repair model in sheep. J Bone Joint Surg Am. 2003;85:2391–402.

8. Turner AS, Athanasiou KA, Zhu CF, Alvis MR, Bryant HU. Biochemical effects of estrogen on articular cartilage in ovariectomized sheep. Osteoarthritis Cartilage. 1997;5:63–9.

9. Johnson J, von Stade D, Regan D, Easley J, Chow L, Dow S, et al. Enthesis trauma as a means for the development of translatable chronic rotator cuff degeneration in an ovine model. Ann Transl Med. 2021;9:741.

10. Easley J, Johnson J, Regan D, Hackett E, Romeo AA, Schlegel T, et al. Partial infraspinatus tendon transection as a means for the development of a translational ovine chronic rotator cuff disease model. Vet Comp Orthop Traumatol. 2020;33:212–9.

11. Turner AS. Experiences with sheep as an animal model for shoulder surgery: strengths and shortcomings. J Shoulder Elbow Surg. 2007;16:S158–63.

12. Kol A, Arzi B, Athanasiou KA, Nolta JA, Rebhun RB, Chen X, et al. Companion animals: translational scientist's new best friends. Sci Transl Med. 2015;7:1–8.

13. Gurr E, Mohr W, Pallasch G. Proteoglycans from human articular cartilage: the effect of joint location on the structure. J Clin Chem Clin Biochem. 1985;23:811–9.

14. Garcia-Seco E, Wilson DA, Cook JL, Kuroki K, Kreeger JM, Keegan KG. Measurement of articular cartilage stiffness of the femoropatellar, tarsocrural, and metatarsophalangeal joints in horses and comparison with biochemical data. Vet Surg. 2005;34:571–8.

15. Changoor A, Hurtig MB, Runciman RJ, Quesnel AJ, Dickey JP, Lowerison M. Mapping of donor and recipient site properties for osteochondral graft reconstruction of subchondral cystic lesions in the equine stifle joint. Equine Vet J. 2006;38:330–6.

16. Frisbie DD, Cross MW, McIlwraith CW. A comparative study of articular cartilage thickness in the stifle of animal species used in human pre-clinical studies compared to articular cartilage thickness in the human knee. Vet Comp Orthop Traumatol. 2006;19:142–6.

17. Malda J, de Grauw JC, Benders KE, Kik MJ, van de Lest CH, Creemers LB, et al. Of mice, men and elephants: the relation between articular cartilage thickness and body mass. PLoS ONE. 2013;8:e57683.

18. Chubinskaya S, Cotter EJ, Frank RM, Hakimiyan AA, Yanke AB, Cole BJ. Biologic characteristics of shoulder articular cartilage in comparison to knee and ankle articular cartilage from individual donors. Cartilage. 2021;12:456–67.

19. Risch M, Easley JT, McCready EG, Troyer KL, Johnson JW, Gadomski BC, et al. Mechanical, biochemical, and morphological topography of ovine knee cartilage. J Orthop Res. 2021;39:780–7.

20. Taylor SD, Tsiridis E, Ingham E, Jin Z, Fisher J, Williams S. Comparison of human and animal femoral head chondral properties and geometries. Proc Inst Mech Eng H. 2012;226:55–62.

21. Martini L, Fini M, Giavaresi G, Giardino R. Sheep model in orthopedic research: a literature review. Comp Med. 2001;51:292–9.

22. Ahern BJ, Parvizi J, Boston R, Schaer TP. Preclinical animal models in single site cartilage defect testing: a systematic review. Osteoarthritis Cartilage. 2009;17:705–13.

23. Changoor A, Fereydoonzad L, Yaroshinsky A, Buschmann MD. Effects of refrigeration and freezing on the electromechanical and biomechanical properties of articular cartilage. J Biomech Eng. 2010;132:064502.

24. Rozen B, Brosh T, Salai M, Herman A, Dudkiewicz I. The effects of prolonged deep freezing on the biomechanical properties of osteochondral allografts. Cell Tissue Bank. 2009;10:27–31.

25. Bansal PN, Joshi NS, Entezari V, Grinstaff MW, Snyder BD. Contrast enhanced computed tomography can predict the glycosaminoglycan content and biomechanical properties of articular cartilage. Osteoarthritis Cartilage. 2010;18:184–91.

26. Farndale RW, Buttle DJ, Barrett AJ. Improved quantitation and discrimination of sulphated glycosaminoglycans by use of dimethylmethylene blue. Biochim Biophys Acta. 1986;883:173–7.

27. Oke SL, Hurtig MB, Keates RA, Wright JR, Lumsden JH. Assessment of three variations of the 1,9-dimethylmethylene blue assay for measurement of sulfated glycosaminoglycan concentrations in equine synovial fluid. Am J Vet Res. 2003;64:900–6.

28. Park S, Hung CT, Ateshian GA. Mechanical response of bovine articular cartilage under dynamic unconfined compression loading at physiological stress levels. Osteoarthritis Cartilage. 2004;12:65–73.

29. Lippiello L, Hall D, Mankin HJ. Collagen synthesis in normal and osteoarthritic human cartilage. J Clin Invest. 1977;59:593–600.

30. Venn M, Maroudas A. Chemical composition and swelling of normal and osteoarthrotic femoral head cartilage. I. Chemical composition. Ann Rheum Dis. 1977;36:121–9.

31. Bland JM, Altman DG. Calculating correlation coefficients with repeated observations: part 1—correlation within subjects. BMJ (Clinical Research Ed). 1995;310:446.

32. Landis JR, Koch GG. The measurement of observer agreement for categorical data. Biometrics. 1977;33:159–74.

33. Bédouet L, Pascale F, Bonneau M, Wassef M, Laurent A. In vitro evaluation of (S)-ibuprofen toxicity on joint cells and explants of cartilage and synovial membrane. Toxicol In Vitro. 2011;25:1944–52.

34. Graichen H, Jakob J, von Eisenhart-Rothe R, Englmeier KH, Reiser M, Eckstein F. Validation of cartilage volume and thickness measurements in the human shoulder with quantitative magnetic resonance imaging. Osteoarthritis Cartilage. 2003;11:475–82.

35. Zumstein V, Kraljević M, Conzen A, Hoechel S, Müller-Gerbl M. Thickness distribution of the glenohumeral joint cartilage: a quantitative study using computed tomography. Surg Radiol Anat. 2014;36:327–31.

36. Zumstein V, Kraljević M, Müller-Gerbl M. Glenohumeral relationships: subchondral mineralization patterns, thickness of cartilage, and radii of curvature. J Orthop Res. 2013;31:1704–7.

37. Schleich C, Bittersohl B, Antoch G, Krauspe R, Zilkens C, Kircher J. Thickness distribution of glenohumeral joint cartilage: a normal value study on asymptomatic volunteers using 3-Tesla magnetic resonance tomography. Cartilage. 2016;8:105–11.

38. Fox JA, Cole BJ, Romeo AA, Meininger AK, Williams JM, Glenn RE Jr, *et al*. Articular cartilage thickness of the humeral head: an anatomic study. Orthopedics. 2008;31:216.

39. Yeh L, Kwak S, Kim Y-S, Chou DS, Muhle C, Skaf A, *et al*. Evaluation of articular cartilage thickness of the humeral head and the glenoid fossa by MR arthrography: anatomic correlation in cadavers. Skeletal Radiol. 1998;27:500–4.

40. Ruckstuhl H, Krzycki J, Petrou N, Vanwanseele B, Stussi E. A quantitative study of humeral cartilage in individuals with spinal cord injury. Spinal Cord. 2008;46:129–34.

41. Appleyard RC, Burkhardt D, Ghosh P, Read R, Cake M, Swain MV, *et al*. Topographical analysis of the structural, biochemical and dynamic biomechanical properties of cartilage in an ovine model of osteoarthritis. Osteoarthritis Cartilage. 2003;11:65–77.

42. Pflieger I, Stolberg-Stolberg J, Foehr P, Kuntz L, Tübel J, Grosse CU, *et al*. Full biomechanical mapping of the ovine knee joint to determine creep-recovery, stiffness and thickness variation. Clin Biomech (Bristol, Avon). 2019;67:1–7.

43. Shepherd DE, Seedhom BB. Thickness of human articular cartilage in joints of the lower limb. Ann Rheum Dis. 1999;58:27–34.

44. Rogers BA, Murphy CL, Cannon SR, Briggs TW. Topographical variation in glycosaminoglycan content in human articular cartilage. J Bone Joint Surg Br. 2006;88:1670–4.

45. Franz T, Hasler M, Hagg R, Weiler C, Jakob RP, Mainil-Varlet P. In situ biomechanical composition, and structural integrity of articular cartilage of the human knee joint. Osteoarthritis Cartilage. 2001;9:582–92.

46. Loy BN, Zimel M, Gowda AL, Tooley TR, Maerz T, Bicos J, *et al*. A biomechanical and structural comparison of articular cartilage and subchondral bone of the glenoid and humeral head. Orthop J Sports Med. 2018;6(7). doi:10.1177/2325967118785854.

47. Huang C-Y, Stankiewicz A, Ateshian GA, Mow VC. Anisotropy, inhomogeneity, and tension-compression nonlinearity of human glenohumeral cartilage in finite deformation. J Biomech. 2005;38:799–809.

48. Patel JM, Wise BC, Bonnevie ED, Mauck RL. A systematic review and guide to mechanical testing for articular cartilage tissue engineering. Tissue Eng Part C Methods. 2019;25:593–608.

49. Lu XL, Mow VC. Biomechanics of articular cartilage and determination of material properties. Med Sci Sports Exerc. 2008;40:193–9.